



# Detection of Epilepsy through Machine Learning Algorithms Using Brain Signals

<sup>1</sup>Dr. P.Jeba Santhiya, <sup>2</sup>J.Rajalakshmi, <sup>3</sup>Dr.S.Siva Ranjani, <sup>4</sup>Dr.'S.ArunMozhi Selvi

<sup>1</sup>Assistant professor

Department of Computer Science and Engineering  
Holy Cross Engineering College, Thoothukudi, Tamil Nadu, India

[jebasanthiya@gmail.com](mailto:jebasanthiya@gmail.com)

<sup>2</sup>Research scholar,

Department of Computer Science and  
EngineeringSethu Institute of Technology,  
Kariyapatti, Virudhunagar, Tamil Nadu, India

[lakshmiyepal@gmail.com](mailto:lakshmiyepal@gmail.com)

<sup>3</sup>Professor

Department of Computer Science and  
EngineeringSethu Institute of Technology,  
Kariyapatti, Virudhunagar, Tamil Nadu, India

[sivaranjani222@gmail.com](mailto:sivaranjani222@gmail.com)

<sup>4</sup>Professor

Department of Computer Science and Engineering  
Holy Cross Engineering College, Thoothukudi, Tamil Nadu, India

[drarunmozhiselvi@gmail.com](mailto:drarunmozhiselvi@gmail.com)

## Abstract

Due to the fact that most seizures in persons with epilepsy occur seldom, it is critical for the classification and diagnosis of epilepsy that the EEG be used. When it comes to adult patients, empirical interpretation of a first EEG is quite insensitive, with sensitivities between 29 and 55% [29–55 percent]. During seizure-free EEG epochs, useful EEG data is buried within the signals, out of reach of any specialised physician in this area who is trained in EEG analysis. We develop a multi-variate strategy to understand the functional connectivity of the brain at the sensor level using EEG data in order to identify individuals with generalized epilepsy, in contrast to the majority of previous studies. Eight different connection characteristics were examined using five different measures across the temporal, periodic, and time-frequency domains. After evaluating the solution using the K-Nearest Neighbour approach, the results were compared to an epilepsy group, and subsequently to a group of patients who had non-epileptic episodes. Classification accuracy (89%) was achieved for EG and HC, however substantial spatial-temporal deficits in the front central areas in the beta frequency band were found in the EG group compared to the HC group. Because of the well-documented coexistence of NEAD and epileptic episodes, the classification accuracy for EG and NEAD was only around 79%. People with specialised epilepsy may be consistently distinguished from those with HC using seizure-free EEG data, according to this research. Although additional study is required in this area to establish a diagnostic tool that is therapeutically helpful,

6011

**Keywords:** Epilepsy, EEG, Brain Signals, Nero Machine Learning, Health care, K-Nearest Neighbour

DOI Number:10.14704/nq.2022.20.8.NQ44628

NeuroQuantology2022;20(8):6011-6018



## Introduction

Epileptic seizure identification research began in the 1970s, and different approaches to this topic have been given. The time-domain technique described by Liu et al. seeks for regular, time signatures in EEG comparable to those seen since movement disorders. The authors used EEG autocorrelation to produce a measure of pacemaker cells [1]. Seizure identification with in frequency response is based on variations in the frequency-domain characteristics of regular and transient EEGs[2].

Because the EEG is non-stationary by nature, time–frequency domain techniques such as wavelet transforms (WT) [3] are best suited because they do not enforce the quasi-stationarity condition on the information like time- and bandwidth approaches. WT gives both temporal and frequency perspectives of a signal at the same time, allowing it to reliably capture and locate transitory elements in data such as seizure spikes. Nonlinear measurements of time series complexity include correlation dimension (CD), maximum Lyapunov exponent (LLE), and ApEn[4]. These measurements aid in understanding EEG dynamics and the original chaos in brain signals [5]. ApEn is just a statistical measure that is commonly utilised in physiological features extraction, such as estimating consistency in epileptic fit data sets [6]. Diambra et demonstrated that the ApEn level lowers dramatically throughout epileptic operations due to its synchronised firing of large neurones. As a result, it is an appropriate characteristic for characterising EEGs. Employed CD to describe interictal EEG for seizure forecast and discovered that CD scores estimated from epileptic EEG data are much lower again for lesion than other parts of the brain [7].

In the last twenty years, artificial neural networks (ANN) have frequently used to categorise EEG data [12–14]. A number of alternative ANN-based techniques for epileptic seizure identification have been reported in the literature [8] employed wavelet transform to capture distinctive aspects of EEG data, which they then integrated with ANN to get a

satisfactory arrangement result. Nigam and colleagues. [9] Developed a technique for automatically detecting epileptic seizures from EEG recordings by employing a multistage regressive pre-processing filter to extract two features: relative spike amplitude and spike occurrence frequency. These characteristics were put into an artificial neural network for diagnosis. [10] Employed short-time fourier transform analysis of EEG data to extract factor based on the pseudo-Wigner–Ville and smoothed-pseudo-Wigner–Ville distributions, which they then fed into an ANN for classification.

For patients with epilepsy, seizure detection may help to better document seizures, which is an important marker for how severe the condition is. This, in turn, could help to distinguish between seizures and other types of events like psychogenic non-epileptic seizures [11]. SUDEP (sudden unexpected death in epilepsy) may be prevented if seizures are detected and alarms are set off. It is impossible to manually analyse long-term digital information such as subcutaneously implanted electroencephalography (EEG) hence automatic seizure identification is particularly significant in these cases.

Though, smaller exploratory investigations are needed to examine the effectiveness and practicality of seizure detection devices and algorithms before larger multi-centre clinical validation studies can be conducted with many patients and seizures. A mixture of ECG, ACM, and behind-the-ear EEG for nonstop offline seizure recognition is the focus of this work.

## 2. Background

### Pre-processing of Data

For all bipolar channels, normalised has to be done on every segment between range from -1 to 1 for each of the four bipolar channels. This phase was carried out only for the purpose of visualisation at the beginning of this study in order to look for any potential artefacts. It has no effect on any of the connection measurements presented in this research [12]. For the purpose of representing

the functional connectivity of the brain between two EEG signals  $x_i$  and  $y_i$ , this study develops five distinct dealings in the time, frequency, and time-frequency fields. These measurements, along with their extensions, are then used to generate classification features.

### Mutual Information

This measure of mutual reliance between 2 signals, i.e., amount of data is transferred between them, is referred to as Mutual Information (MI). It is created on the entropy and probability function of this situation. Entropy is defined as the amount of variation in a signal X throughout its length n as shown in Eq. (1).

$$G(x) = \sum_{i=1}^n (x_i) \log p(x_i) \quad - \quad (1)$$

### Correlation

As the name implies, this well-known metric illustrates how two signals are linked with one another when there is a temporal shift between the two signals. The cross-correlation coefficients utilised in this investigation were computed using the following formula in Eq. (2)

$$H_{xy}[n] = \frac{\sum_{j=-\infty}^{\infty} [l+y[l+1]]}{\sqrt{\sum_{j=-\infty}^{\infty} x[l]^2} \sqrt{\sum_{j=-\infty}^{\infty} y[l+1]^2}} \quad (2)$$

The properties of the cross correlation that are extracted: the greatest correlation value, the mean correlation value, and the correlation lag when the maximum correlation value is obtained. The properties must be noted that while computing the correlation's highest value and correlation's approximation is also considered. This is because two EEG signals may potentially be negatively correlated with one another.

## Detection of seizures processing and characteristics of EEG data

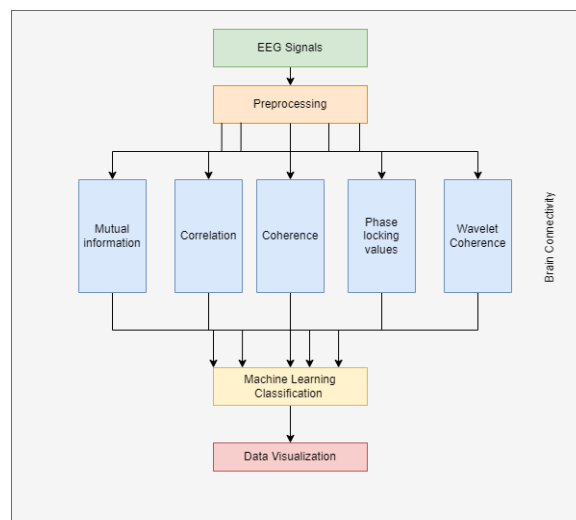


Fig.1 Proposed model

An EEGLAB toolbox and scripts were utilised to input data into EEGLAB. The cross channel between the two ears and the channels from the left and right ears were both used as references. The data is segmented into two-epochs were the frequency ranges that were culled from the signal.

6013

MATLAB's spectrum analyser function and a short-time Fourier transform were used to create the time-frequency-power graphs for the visuals. A finite impulse response band pass filter with a 1–70 Hz frequency range and a 50 Hz frequency range stop filter were used for time-domain visualisations of the unsegmented EEG. The technique used to compute the variance has been previously explained. To ensure that the plots were devoid of artefacts and stereotyped seizures, they were carefully selected.

### Using Support vector Machine

A patient-specific SVM classifier is trained on each patient separately and exclusively on affected role with at least six verified seizures. The classifier utilised all seizures since these individuals, regardless of signal quality or ictal changes shown in the data. Classification was done using an SVM with radial common function kernel. To adjust for class imbalance, the Synthetic Minority Oversampling Method [1] was used with three



resampling rounds. The classifier was running separately with all modes, EEG & ACM, EEG & ACM, and simply EEG. Everyone's features are resampled. Each patient's data was divided into folds, one for each seizure, with fold borders corresponding to the centre point between them. Each fold included confiscation and non-seizure data.

After creating a random seed for repeatability, the algorithm is skilled on one-fold fewer folds than the total amount. The other fold was used as a trial run. " Seizures and non-seizures were predicted by the classifier for each sample from the 1's windows. A single sample was foreseen to be either "seizure" or "non-seizure" while the previous and subsequent samples were anticipated to be the other. A smallest seizure duration (MSD) criterion was established once each seizure or non-seizure sample was found. To limit sensitivity and reduce FAR, we raised the MSD threshold value. In the process of obtaining the classifier's Receiver Operating Characteristic (ROC), it ranged from 5 to 60 seconds (in 5 second increments).

To prevent numerous alarms for the same event, a 2-minute refractory delay was imposed after each positive detection. To accommodate for modest synchronisation errors, a projected seizure was judged accurate if it occurred in 50 s of the EEG onset-offset period. The classifier's sensitivity and false detection rates (FAR) were calculated for each test fold and averaged across all test folds weighted by its durations.

### 3 Experimental Results

The study comprised 40 patients (23 male, ages 19–77, median 43). One focal to bilateral generalised tonicclonic seizure was documented from one sick person while in the EMU. SVM was assigned to three people who had more than five seizures. (Enobio 73 percent range: 25–100%; TrackIT 99.6% range: 93–100%). Fig. 1 depicts patient recording time. Technical issues caused the majority of closed-ear EEG loss. Technical issues lost ECG data for two non-seizures. 57 seizures were lost due to battery exhaustion, but the ECG gadget caught ACM in all seven. So the SENS ACM

data was left out. All patients completed the desired monitoring time.

**Table 1 Various parameters of analysing EEG**

Variable	Predicting models	P <sup>2</sup>	hf <sub>m</sub>	hf <sub>r</sub>	M	Q	ΔZ
Step 1	Education, age, epilepsy duration,	0.42	4	39	6.93	<0.001	0.41
Step 2	Pictur naming	0.52	1	38	8.21	0.006	0.10
Step 3	Education, AED number	0.56	1	37	3.41	0.058	0.04

6014

### Nonmotor focal seizures

Seizures begin in the temporal lobe, median duration 53 s (range 42–73 s). There were lip smacking and gazing as well as oral automatisms. The patient was conscious of four of five awoken seizures. The patient experienced an actual rise in HR, 110 BPM median peak HR, 93–121 BPM range, and significant alterations in HRV, as seen in Fig. 2 and Fig.3, indicating potential seizure episodes and incidence of seizure patients admitted.

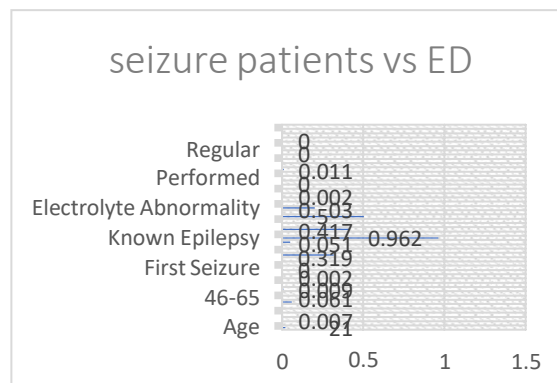


Fig.2 Seizure patients hospitalised to the emergency department (ED) and their frequency of admission

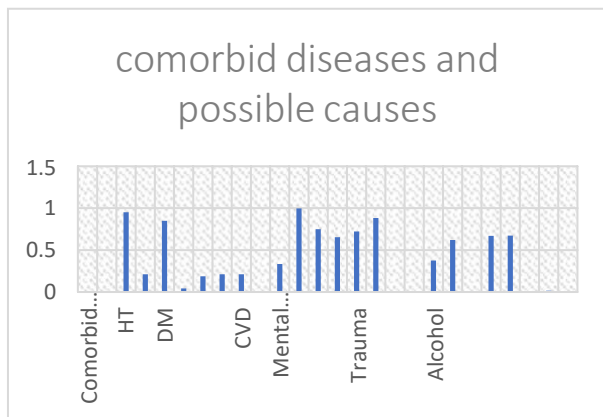


Fig.3 The incidence of seizure patients admitted to the ED and their concomitant conditions.

### Results of SVM classification

The three patients' RCCs were drawn for threshold values of MSD parameters (6–60 s). First epilepsy patient within nonmotor focal seizures (patient 3) had 100% sensitivity and the EEG/ECG combo has the best sensitivity across most MSD levels.

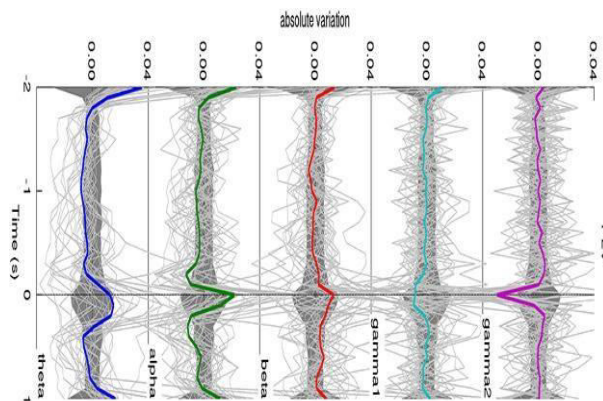


Fig.4 Patient 18 had 11 focal tonic seizures in a 19-hour period.

A signal indicates a seizure. HRV vary in synchronisation through seizures. Notably, most non-ictal variance or HRV oscillations are not coordinated. Fig.4 shows patient record in 19-hour period and some seizures display movement on accelerometry. Time-domain representation of a seizure. Time-domain graphs from patient 19 through EEG (channel: T9-T10) from an epilepsy monitoring device

during the same event. The pulse rate increases from 50 BPM to 100 BPM 15 seconds after the episode ends.

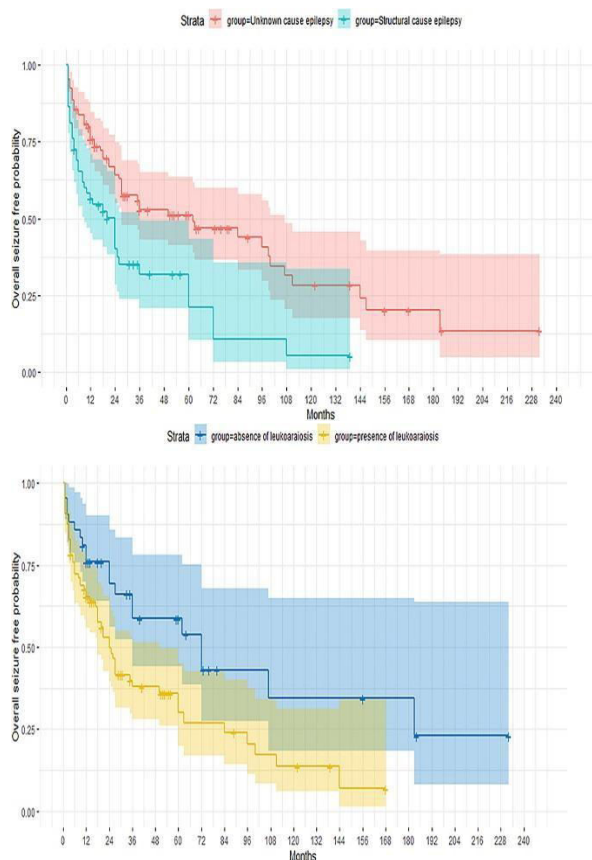


Fig.5 ROC signal of the personalised automated seizure detection system.

Patient 4 experienced nine focal nonmotor seizures. EEG and ECG with a 40 s minimum seizure length threshold recognised all seizures with a 13/24 false alarm rate. Fig.5 shows ROC signal of the personalised automated seizure detection system with A 25 s threshold gave 84% understanding and a FAR of 8/24 h. No motor seizures in patient 26. EEG and ECG with a 35 s MSD threshold found all 5/24 h FAR seizures In certain circumstances, two MSD thresholds provided equivalent or overlapping sensitivity and FAR.

### 4. Conclusion

This article investigated the efficacy of a specialised multimodal seizure detection technics that could be used both automatically and manually to examine the data. The performance of an proposed automated seizure detection using SVM based procedure



employing various multi-modal combinations within ACCM, ECG, and EEG was superior to that of a uni-modal EEG method when compared to the uni-modal EEG. EEG and ECG derived characteristics may be used to augment manual data evaluation of recordings by giving an outline of seizure suspect epochs within the previously recorded data, which can be helpful in identifying seizure suspicious epochs within the recorded data.

## References

- [1] M. Pievani, et al., Functional network disruption in the degenerative dementias, *Lancet Neurol.* 10 (9) (2011) 829–843, [https://doi.org/10.1016/S1474-4422\(11\)70158-2](https://doi.org/10.1016/S1474-4422(11)70158-2).
- [2] F. Varela, et al., The brainweb: phase synchronization and large-scale integration, *Nat. Rev. Neurosci.* 2 (4) (2001) 229–239, <https://doi.org/10.1038/35067550>.
- [3] V. Brodbeck, et al., EEG microstates of wakefulness and NREM sleep, *NeuroImage* 62 (3) (2012) 2129–2139, <https://doi.org/10.1016/j.neuroimage.2012.05.060>.
- [4] G. Lioi, et al., Directional connectivity in the EEG is able to discriminate wakefulness from NREM sleep, *Physiol. Meas.* 38 (9) (2017) 1802–1820, <https://doi.org/10.1088/1361-6579/aa81b5>.
- [5] G.K. Dash, et al., Interictal regional paroxysmal fast activity on scalp EEG is common in patients with underlying gliosis, *Clin. Neurophysiol.* 129 (5) (2018) 946–951, <https://doi.org/10.1016/j.clinph.2018.02.007>.
- [6] R. Renzel, et al., Persistent generalized periodic discharges: a specific marker of fatal outcome in cerebral hypoxia, *Clin. Neurophysiol.* 128 (1) (2017) 147–152, <https://doi.org/10.1016/j.clinph.2016.10.091>.
- [7] H. Watanabe, et al., Effect of hyperventilation on seizures and EEG findings during routine EEG, *Clin. Neurophysiol.* 129 (5) (2018) e38, <https://doi.org/10.1016/j.clinph.2018.02.097>.
- [8] Arends J, Thijs RD, Gutter T, Ungureanu C, Cluitmans P, Van Dijk J, et al. Multimodal nocturnal seizure detection in a residential care setting: A long-term prospective trial. *Neurology* 2018;91(21):e2010–9.
- [9] Beck M, Simony C, Zibrandtsen I, Kjaer TW. Readiness among people with epilepsy to carry body-worn monitor devices in everyday life: A qualitative study. *Epilepsy Behav* 2020;112:107390. <https://doi.org/10.1016/j.yebeh.2020.107390>.
- [10] Beniczky S, Jeppesen J. Non-electroencephalography-based seizure detection. *Curr Opin Neurol* 2019;32(2):198–204.
- [11] Beniczky S, Ryvlin P. Standards for testing and clinical validation of seizure detection devices. *Epilepsia* 2018;59:9–13.
- [12] Beniczky S, Wiebe S, Jeppesen J, Tatum WO, Brazdil M, Wang Y, et al. Automated seizure detection using wearable devices: A clinical practice guideline of the International League Against Epilepsy and the International Federation of Clinical Neurophysiology. *Epilepsia* 2021;62(3):632–46.
- [13] Boonyakitanont P, Lek-uthai A, Chomtho K, Songsiri J. A review of feature extraction and performance evaluation in epileptic seizure detection using EEG. *Biomed Signal Process Control* 2020;57:101702. <https://doi.org/10.1016/j.bspc.2019.101702>.
- [14] Bouchequet P. rsleep: Analysis of Sleep Data. R package version 1.0.3. 2020. Available from: <https://CRAN.R-project.org/package=rsleep>.
- [15] Taylor JP, Hardy J, Fischbeck KH. Toxic proteins in neurodegenerative disease. *Science* 2002; 296: 1991–95.
- [16] Ikonovic MD, Klunk WE, Abrahamson EE, et al. Post-mortem correlates of in vivo PiB-PET amyloid imaging in a typical case of Alzheimer’s disease. *Brain* 2008; 131: 1630–45.



- [17] Whitwell JL, Josephs KA, Murray ME, et al. MRI correlates of neurofibrillary tangle pathology at autopsy: a voxel-based morphometry study. *Neurology* 2008; 71: 743–49.
- [18] McKhann GM, Knopman DS, Chertkow H, et al. The diagnosis of dementia due to Alzheimer’s disease: recommendations from the National Institute on Aging-Alzheimer’s Association workgroups on diagnostic guidelines for Alzheimer’s disease. *Alzheimers Dement* 2011; 7: 263–69.
- [19] Albert MS, Dekosky ST, Dickson D, et al. The diagnosis of mild cognitive impairment due to Alzheimer’s disease: recommendations from the National Institute on Aging-Alzheimer’s Association workgroups on diagnostic guidelines for Alzheimer’s disease. *Alzheimers Dement* 2011; 7: 270–79.
- [20] Seeley WW, Crawford R, Rascofsky K, et al. Frontal paralimbic network atrophy in very mild behavioral variant frontotemporal dementia. *Arch Neurol* 2008; 65: 249–55.
- [21] Whitwell JL, Josephs KA. Voxel-based morphometry and its application to movement disorders. *Parkinsonism Relat Disord* 2007; 13 (suppl 3): S406–16.
- [22] Whitwell JL, Weigand SD, Shiung MM, et al. Focal atrophy in dementia with Lewy bodies on MRI: a distinct pattern from Alzheimer’s disease. *Brain* 2007; 130: 708–19.
- [23] Du AT, Schuff N, Kramer JH, et al. Different regional patterns of cortical thinning in Alzheimer’s disease and frontotemporal dementia. *Brain* 2007; 130: 1159–66.
- [24] Frisoni GB, Fox NC, Jack CR Jr, Scheltens P, Thompson PM. The clinical use of structural MRI in Alzheimer disease. *Nat Rev Neurol* 2010; 6: 67–77.
- [25] Alladi S, Xuereb J, Bak T, et al. Focal cortical presentations of Alzheimer’s disease. *Brain* 2007; 130: 2636–45.
- [26] Sporns O. The human connectome: a complex network. *Ann N Y Acad Sci* 2011; 1224: 109–25.
- [27] Stam CJ. Use of magnetoencephalography (MEG) to study functional brain networks in neurodegenerative disorders. *J Neurol Sci* 2010; 289: 128–34.
- [28] Bullmore E, Sporns O. Complex brain networks: graph theoretical analysis of structural and functional systems. *Nat Rev Neurosci* 2009; 10: 186–98.
- [29] Zhang D, Raichle ME. Disease and the brain’s dark energy. *Nat Rev Neurol* 2010; 6: 15–28.
- [30] Sperling RA, Dickerson BC, Pihlajamaki M, et al. Functional alterations in memory networks in early Alzheimer’s disease. *Neuromolecular Med* 2010; 12: 27–43.
- [31] Bokde AL, Ewers M, Hampel H. Assessing neuronal networks: understanding Alzheimer’s disease. *Prog Neurobiol* 2009; 89: 125–33.
- [32] Sorg C, Riedl V, Pernecky R, Kurz A, Wohlschlagel AM. Impact of Alzheimer’s disease on the functional connectivity of spontaneous brain activity. *Curr Alzheimer Res* 2009; 6: 541–53.
- [33] Dickerson BC, Sperling RA. Large-scale functional brain network abnormalities in Alzheimer’s disease: insights from functional neuroimaging. *Behav Neurol* 2009; 21: 63–75.
- [34] Guye M, Bettus G, Bartolomei F, Cozzone PJ. Graph theoretical analysis of structural and functional connectivity MRI in normal and pathological brain networks. *MAGMA* 2010; 23: 409–21.
- [35] Dickerson BC. Advances in functional magnetic resonance imaging: technology and clinical applications. *Neurotherapeutics* 2007; 4: 360–70.
- [36] He Y, Chen Z, Evans A. Structural insights into aberrant topological patterns of large-scale cortical networks in Alzheimer’s disease.



J Neurosci 2008; 28: 4756–66.

[37] Yao Z, Zhang Y, Lin L, Zhou Y, Xu C, Jiang T; Alzheimer’s Disease Neuroimaging Initiative. Abnormal cortical networks in mild cognitive impairment and Alzheimer’s disease. PLoS Comput Biol 2010; 6: e1001006.

[38] Fox MD, Raichle ME. Spontaneous fluctuations in brain activity observed with functional magnetic resonance imaging. Nat Rev Neurosci 2007; 8: 700–11.

[39] Beckmann CF, DeLuca M, Devlin JT, Smith SM. Investigations into resting-state connectivity using independent component analysis. Philos Trans R Soc Lond B Biol Sci 2005; 360: 1001–13.

[40] Damoiseaux JS, Rombouts SA, Barkhof F, et al. Consistent resting-state networks across healthy subjects. Proc Natl Acad Sci USA 2006; 103: 13848–53.

